Annu. Rev. Biochem. 2019.88:365-381. Downloaded from www.annualreviews.org
Access provided by University of California - San Francisco UCSF on 06/24/19. For personal use only.

Annual Review of Biochemistry

Lysine-Targeted Inhibitors and Chemoproteomic Probes

Adolfo Cuesta and Jack Taunton

Department of Cellular and Molecular Pharmacology, University of California, San Francisco, California 94158, USA; email: Adolfo.cuesta@ucsf.edu, Jack.taunton@ucsf.edu

Annu. Rev. Biochem. 2019. 88:365–81

First published as a Review in Advance on January 11, 2019

The *Annual Review of Biochemistry* is online at biochem.annualreviews.org

https://doi.org/10.1146/annurev-biochem-061516-044805

Copyright © 2019 by Annual Reviews.
All rights reserved

Keywords

aldehyde, sulfonyl fluoride, chemoproteomics, kinase, reversible covalent

Abstract

Covalent inhibitors are widely used in drug discovery and chemical biology. Although covalent inhibitors are frequently designed to react with noncatalytic cysteines, many ligand binding sites lack an accessible cysteine. Here, we review recent advances in the chemical biology of lysine-targeted covalent inhibitors and chemoproteomic probes. By analyzing crystal structures of proteins bound to common metabolites and enzyme cofactors, we identify a large set of mostly unexplored lysines that are potentially targetable with covalent inhibitors. In addition, we describe mass spectrometry–based approaches for determining proteome-wide lysine ligandability and lysine-reactive chemoproteomic probes for assessing drug–target engagement. Finally, we discuss the design of amine-reactive inhibitors that form reversible covalent bonds with their protein targets.

Contents

Annu. Rev. Biochem. 2019.88:365-381. Downloaded from www.annualreviews.org
Access provided by University of California - San Francisco UCSF on 06/24/19. For personal use only.

INTRODUCTION

The development of electrophilic small molecules that selectively react with a protein nucleophile is a major focus of chemical biology and drug discovery efforts (1, 2). Covalent inhibitors usually function through a two-step process in which reversible noncovalent binding precedes a reversible or irreversible reaction between an electrophile on the small molecule and a proximal nucleophile on the protein target. Covalent bond formation can result in sustained target engagement (slow off-rate, long drug–target residence time) and increased pharmacodynamic potency in vivo. After an irreversible covalent drug has been administered, recovery of the target's function depends on its resynthesis rate rather than the drug clearance rate, potentially resulting in a prolonged duration of action despite rapid clearance (3, 4). In addition, covalent ligands bearing an affinity tag or fluorophore are employed as chemoproteomic probes to quantify drug–target engagement and proteome-wide selectivity (5).

Cysteine is the most intrinsically reactive amino acid, and even noncatalytic cysteines can react rapidly with weak electrophiles if the reacting atoms are optimally oriented. Structure-guided targeting of noncatalytic cysteines is now a prominent strategy in drug discovery. This strategy has led to the discovery of first-in-class inhibitors of protein–protein interactions, exemplified by covalent antagonists of the oncogenic Gly12Cys mutant of KRAS and the nuclear export receptor, XPO1 (6–12). In addition, targeting noncatalytic cysteines has been employed to increase the selectivity of protein kinase inhibitors (13–16), culminating in the recent US Food and Drug Administration approval of covalent inhibitors of the tyrosine kinases EGFR (afatinib, osimertinib), BTK (ibrutinib, acalabrutinib), and HER2 (neratinib) (17–21). A limitation of this approach is that many ligandable sites lack a cysteine residue.

Lysine is one of the most prevalent amino acids in the proteome, with ~650,000 lysine residues distributed among ~20,000 human proteins. By contrast, there are only ~260,000 cysteines, many of which are engaged in structural disulfide bonds and therefore are non-nucleophilic. Aryl sulfonyl fluorides (22–25), aryl fluorosulfates (26, 27), Michael acceptors (28–33), dichlorotriazines (34), activated esters/amides (35–42), and aryl aldehydes (43–47) have been shown to form covalent adducts with lysine residues when added to purified proteins, cell lysates, or intact cells (**Table 1**). However, compared with cysteine-targeted inhibitors, relatively few covalent inhibitors and probes (and no approved drugs) have been designed to target lysine (reviewed in 48). Hence, the lysine ε-amine and, to a lesser extent, the N-terminal amine of certain proteins present a largely unexplored opportunity for covalent targeting [note that only ~20% of human proteins contain an unblocked N-terminal amine (49)]. This opportunity comes with challenges, including low intrinsic nucleophilicity—most lysines are predominantly protonated at physiological pH—and a

selectivity challenge due to the ubiquitous distribution of lysines throughout the proteome, with each protein having 32 lysines on average. Although certain lysines are more intrinsically reactive than others (e.g., owing to microenvironment-perturbed pK_a), identification of such lysines by computational prediction or empirical approaches is challenging. In this review, we discuss strategies for (*a*) identifying ligandable lysines in proteins and proteomes and (*b*) developing lysine-targeted covalent inhibitors and chemoproteomic probes.

MINING THE PROTEIN DATA BANK FOR LIGANDABLE LYSINES

Structural analysis, along with empirical studies using chemoproteomic probes, suggests that each of the >500 human protein kinases has an active-site lysine that can react with a covalent inhibitor. To expand this analysis to other protein classes, we searched the Protein Data Bank (PDB) for lysines in close proximity to the following metabolites (and stable analogs), which are widely employed as enzyme substrates, cofactors, and allosteric modulators: ADP/ATP, GDP/GTP, α-ketoglutarate, NAD(P)/NAD(P)H, and S-adenosyl methionine (SAM). We limited our PDB analysis to crystal structures with a resolution of 3 Å or better. Excluding protein kinases, we identified 470 human proteins (on the basis of Uniprot ID) bound to one or more of these metabolites (**Table 2**). Strikingly, ~75% have at least one lysine within 5 Å of the metabolite (measured from the lysine ε-amine). The entire curated list, which includes the Uniprot ID, the bound metabolite,

Table 1 Lysine-reactive electrophiles cited in this review

Name	Electrophile	Lysine adduct	Major nucleophile	Reference(s)
Aryl sulfonyl fluoride	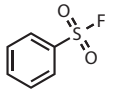	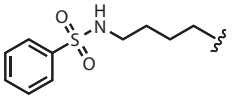	Lysine, tyrosine, serine	22–25
Aryl fluorosulfate	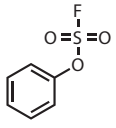	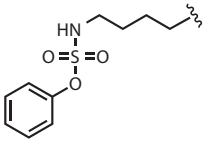	Lysine, tyrosine, serine	26, 27
Vinyl sulfone/ sulfonamide		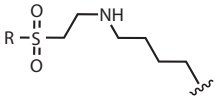	Cysteine, lysine	29, 31
Methyl fumaramide	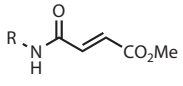	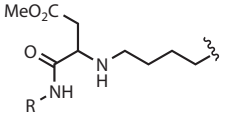	Cysteine, lysine	30, 33
Acrylate	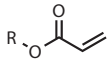	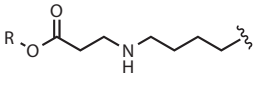	Cysteine, lysine	32
Dichlorotriazine	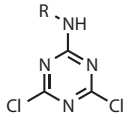	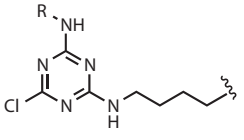	Lysine	34

(*Continued*)

Annu. Rev. Biochem. 2019.88:365-381. Downloaded from www.annualreviews.org
Access provided by University of California - San Francisco UCSF on 06/24/19. For personal use only.

Table 1 (*Continued*)

Name	Electrophile	Lysine adduct	Major nucleophile	Reference(s)
Activated ester/amide	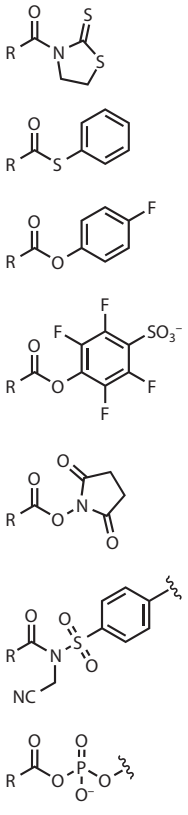	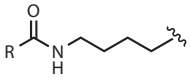	Lysine	35–42
Salicylaldehyde	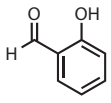	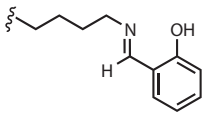	Lysine (N terminus)	43–45
2-Formyl phenyl boronic acid	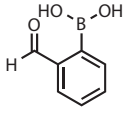	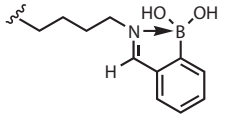	Lysine	46, 47

Table 2 Number of unique human proteins in the Protein Data Bank (excluding kinases) with lysines ≤5 Å from the indicated metabolite

	Number of lysine residues			
	0	**1**	**2**	**≥3**
GTP	3	7	47	38
ATP	24	81	39	12
α-Ketoglutarate	10	24	0	0
NAD(P)/NAD(P)H	23	42	36	10
S-adenosyl methionine	50	23	2	0

Annu. Rev. Biochem. 2019.88:365-381. Downloaded from www.annualreviews.org
Access provided by University of California - San Francisco UCSF on 06/24/19. For personal use only.

Annu. Rev. Biochem. 2019.88:365-381. Downloaded from www.annualreviews.org
Access provided by University of California - San Francisco UCSF on 06/24/19. For personal use only.

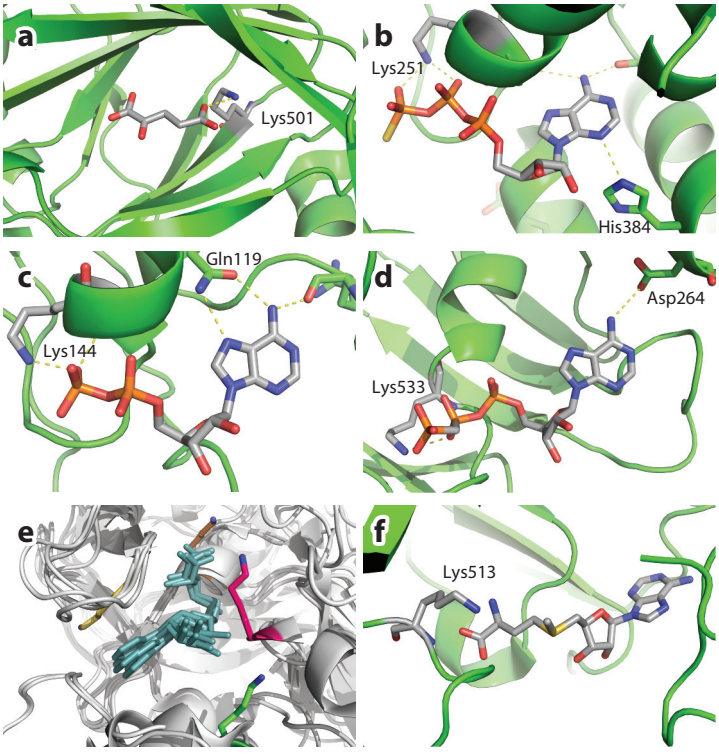

Figure 1

Mining the Protein Data Bank (PDB) for lysines proximal to metabolite/cofactor binding sites. (*a*) A conserved lysine in the Jumonji C demethylase domain of KDM5A interacts with α-ketoglutarate (PDB: 5E6H). (*b–d*) Although a proximal lysine is found in phylogenetically divergent ATPases, they employ distinct ATP binding modes and hydrogen bonding interactions: (*b*) AAA+ ATPase p97/VCP (PDB: 4KO8), (*c*) DEAD-box helicase DDX19 (PDB: 3EWS), and (*d*) mitochondrial ABC transporter ABCB10 (PDB: 4AYT). (*e*) Overlay of four SET domains with spatially distinct lysines proximal to SAM or S-adenosylhomocysteine (*cyan*): KMT5A (*yellow*; PDB: 2BQZ), SETD7 (*orange*; PDB: 3CBM), SUV39H2 (*magenta*; PDB: 2R3A), and EHMT1 (*green*; PDB: 4I51). (*f*) SAM-proximal Lys513 in METTL3, a non-SET domain methyltransferase for N^6-adenosine (PDB: 5IL1).

and the position of the proximal lysine(s), is presented in **Supplemental Table 1**. ATPases and GTPases are highly represented in this group, consistent with the known phosphate-binding and essential catalytic roles of lysine in these enzymes. In addition, most of the identified α-ketoglutarate binding proteins have a lysine that interacts with a carboxylate of the cofactor (e.g., Jumonji C-domain lysine demethylases) (**Figure 1*a***).

Supplemental Material >

Although phylogenetically diverse ATPases employ a conserved lysine to engage one or more phosphate oxygens, these proteins often differ in their fold, active-site structure, and specific interactions with ATP. For example, the AAA+ ATPase p97, DEAD-box helicase DDX19, and ABC transporter ABCB10 contact the β-phosphate of ATP using a similarly positioned lysine (**Figure 1*b–d***). Despite this shared feature, the adenine moiety forms distinct van der Waals and hydrogen bonding interactions with the protein in each case (**Figure 1*b–d***). By exploiting these structural differences in the ATP binding site, it should be possible to design covalent inhibitors that target this lysine yet discriminate among distinct ATPase families.

SET family methyltransferases use SAM to methylate lysine residues on histones, transcription factors, and other proteins. Of the 26 human SET family methyltransferase domains in the PDB, 9 have a lysine at various locations in the SAM binding site (**Figure 1*e***). Targeting a poorly conserved lysine with a SAM-competitive covalent inhibitor could serve as a strategy to increase selectivity among SET family methyltransferases. Outside the SET family, other methyltransferases contain a SAM-proximal lysine, including the N^6-adenosine methyltransferase METTL3, which was recently implicated in acute myeloid leukemia (50, 51) (**Figure 1*f***).

Because we limited our analysis to structurally characterized proteins and a small set of metabolites/cofactors, our findings likely represent the tip of the iceberg in terms of ligandable lysines in the human proteome. To increase the inventory of ligandable lysines, we propose the following: (*a*) structural bioinformatic analysis of all protein structures in the PDB—as well as homologous proteins not in the PDB—with the aim of identifying lysines proximal to all potentially ligandable sites, including allosteric sites and protein–protein interfaces, and (*b*) empirical interrogation of the proteome using lysine-reactive chemical probes.

DETERMINANTS OF LYSINE REACTIVITY AND LIGANDABILITY

In addition to its proximity to a small-molecule binding site, a lysine's intrinsic nucleophilicity is a critical determinant of ligandability governed, in part, by its pK_a. In solution, the pK_a of the protonated ε-amine of lysine is 10.4, whereas in proteins it can range from ∼5 to ∼11 depending on the local microenvironment (e.g., local dielectric, proximity of negatively and positively charged side chains) (52). Although it is difficult to measure, let alone predict, the pK_a of specific lysines, one can measure their relative reactivity toward simple electrophiles using quantitative mass spectrometry. In a recent study, acetyl CoA and acetyl phosphate were used to measure the relative reactivity of 90 lysines across 8 purified proteins. The second-order rate constants spanned three orders of magnitude, with 30% of the lysines being unreactive (53). Decreased reactivity correlated in many cases with ionic interactions between the lysine and a proximal aspartate or glutamate (e.g., ACAT1 Lys84). The most reactive lysines (e.g., GDH Lys503) were on the protein surface, close to other positively charged residues. The increased reactivity of these lysines can be explained by their perturbed pK_a as well as their accessibility to the charged electrophiles. These observations raise a potential caveat to these types of measurements: The reactivity of solvent-exposed surface lysines toward small, charged active esters may not reflect reactivity toward lipophilic, sterically demanding electrophiles. That is, a lysine's intrinsic reactivity may vary depending on the specific physicochemical properties of the test electrophile.

Using advanced chemoproteomic methods, it should be feasible to measure the relative reactivity of every lysine in the proteome toward a model electrophilic probe; in practice, this remains challenging owing to the massive number of lysines. In a recent study (41), proteome-wide lysine reactivity was estimated by treating cell lysates with two concentrations of a clickable lysine-reactive probe, sulfotetrafluorophenyl pentynoate (STP-alkyne) (**Figure 2*a***). A similar study used a clickable *N*-hydroxysuccinimide (NHS) ester as the probe (42). After copper-catalyzed click conjugation to a cleavable biotin azide and affinity purification with streptavidin-agarose beads, probe-modified peptides were identified by mass spectrometry. The difference in labeling intensity between the two probe concentrations was used to infer relative reactivity; lysines with roughly equivalent labeling intensity under both conditions were deemed highly reactive (labeled to saturation at the lower probe concentration), whereas those with increased labeling proportional to the probe concentration were deemed to have moderate or low reactivity. Using this workflow, the reactivity of >4,000 lysines was estimated using proteomes derived from three human cancer cell lines. Hyperreactive lysines (<10% of lysines modified by STP-alkyne) were enriched in enzyme active sites and ligand binding sites.

Annu. Rev. Biochem. 2019.88:365-381. Downloaded from www.annualreviews.org
Access provided by University of California - San Francisco UCSF on 06/24/19. For personal use only.

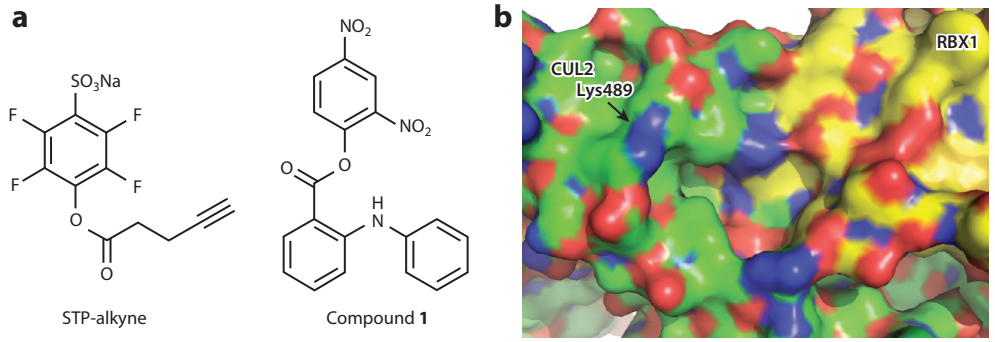

Figure 2

Proteome-wide determination of lysine reactivity and ligandability using the clickable probe sulfotetrafluorophenyl pentynoate (STP-alkyne) and quantitative mass spectrometry. (*a*) Chemical structure of STP-alkyne and reactive ester fragment **1**. Fragment **1** was found to prevent covalent modification of E3 ubiquitin ligase subunit CUL2 at Lys489 by STP-alkyne (41). (*b*) CUL2 Lys489 is adjacent to a pocket at the interface with RBX1 in an E3 ligase complex (Protein Data Bank: 5N4W).

Annu. Rev. Biochem. 2019.88:365-381. Downloaded from www.annualreviews.org
Access provided by University of California - San Francisco UCSF on 06/24/19. For personal use only.

Competition experiments using STP-alkyne and a panel of 32 lysine-reactive fragments (NHS, pentafluorophenyl, and other active esters) were used to identify lysines proximal to saturable fragment binding sites (i.e., ligandable lysines). Only a minor fraction (<2%) of the STP-alkyne–modified lysines were completed by pretreating lysates with one or more active ester fragments. Some of the ligandable lysines were found in challenging, classically undruggable targets, including protein–protein interaction domains. For example, several fragments modified the transcriptional repressor SIN3A at Lys155, which inhibited SIN3A binding to TGIF1, a DNA-binding transcription factor. The data set of 121 ligandable lysines in 113 human proteins can potentially serve as a resource for structure-based design of new covalent probes. As an example, we highlight the E3 ubiquitin ligase subunit CUL2. As shown in the supplementary data set accompanying the Hacker et al. study (41), CUL2 Lys489 was labeled by two active ester fragments, including compound **1** (**Figure 2*a***). A recent crystal structure (54) of a multisubunit E3 ligase complex reveals that CUL2 Lys489 is adjacent to a shallow pocket at the interface of CUL2 and the E2-binding subunit RBX1 (**Figure 2*b***). Covalent modification of this lysine with small-molecule ligands that bind to this interface could potentially inhibit CUL2 E3 ligase activity; alternatively, targeting this site with a bifunctional ligand could be used to promote ubiquitination and degradation of neosubstrates (55–58).

The data set reported by Hacker et al. (41) provides the most comprehensive view of lysine reactivity to date. Nevertheless, it captures only a small fraction of the total number of lysines in the proteome. For example, although STP-alkyne labeled 70 kinases, only 15 probe-modified lysines correspond to the kinase catalytic lysine. By contrast, the catalytic lysine in >300 protein kinases has been shown to react rapidly with active site–directed acyl phosphate and sulfonyl fluoride probes (24, 25, 40). Efficient modification of the kinase catalytic lysine, situated in a deep hydrophobic pocket, may require tailored probes with higher intrinsic affinity for the ATP binding site. We speculate that this may be true for many other ligandable lysines.

CHEMOPROTEOMIC PROBES TARGETING THE CATALYTIC LYSINE IN PROTEIN KINASES

Protein kinases comprise a large family of signal-transducing enzymes (>500 in humans) that regulate all cellular processes. Kinases are validated therapeutic targets for cancer, rheumatoid

arthritis, and idiopathic pulmonary fibrosis, and they continue to be a central focus of drug discovery efforts for many other diseases. In addition to their prominent role as drugs, selective kinase inhibitors often provide new mechanistic insights that are not easily obtained through genetic approaches (59).

Given the highly conserved ATP binding site and the presence of hundreds of kinases in any given cell type, a key question inevitably arises with the use of any kinase inhibitor: When the inhibitor is added to cells at a concentration that induces a phenotype of interest (e.g., cancer cell death), which kinases are occupied by the inhibitor and to what extent? Although selectivity is typically assessed by profiling a panel of purified recombinant kinases or kinase domains, recent chemoproteomic methods have been developed to interrogate hundreds of endogenously expressed kinases in a single experiment, in either cell lysates or intact cells (40, 60, 61). Such methods have the potential advantage of quantifying inhibitor–kinase interactions in a more physiologically relevant context.

ADP- and ATP-desthiobiotin are acyl phosphate–based chemoproteomic probes that were designed to react with a proximal lysine residue in protein kinases and other ATP-utilizing enzymes (39). In protein kinases, the primary modification site is the conserved and catalytically essential lysine, which coordinates the ADP leaving group during the phospho-transfer reaction (**Figure 3*a***).

Annu. Rev. Biochem. 2019.88:365-381. Downloaded from www.annualreviews.org
Access provided by University of California - San Francisco UCSF on 06/24/19. For personal use only.

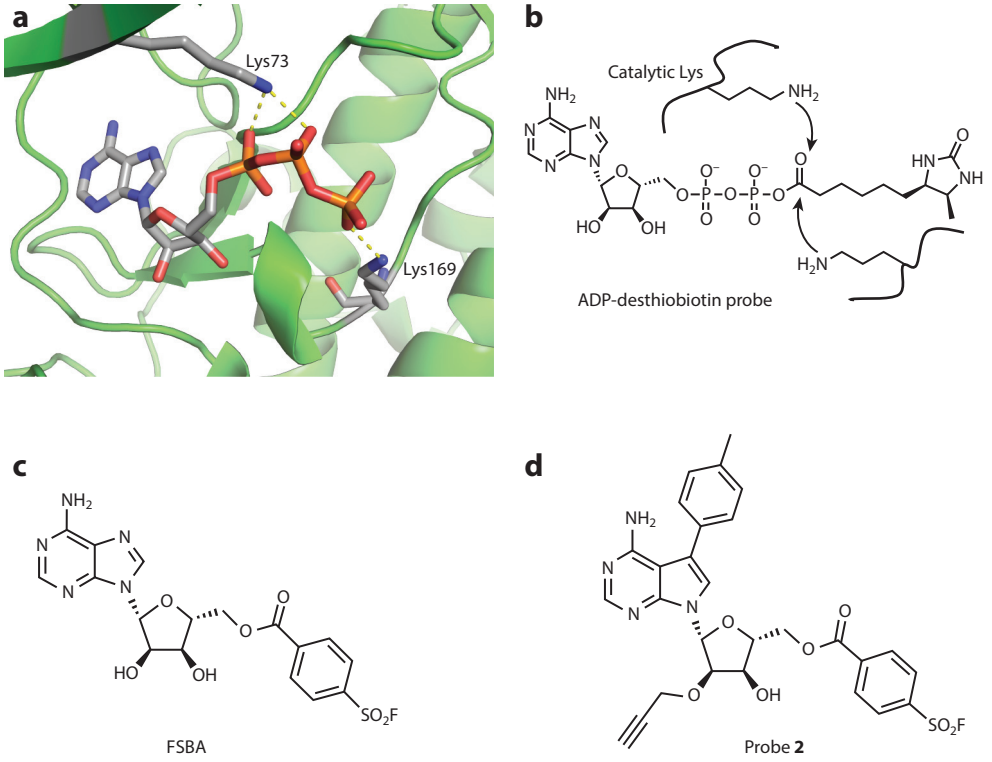

Figure 3

Lysine-targeted chemoproteomic probes for kinases and other ATP binding proteins. (*a*) Crystal structure of protein kinase A bound to ATP showing the conserved catalytic Lys73 and proximal Lys169 (Protein Data Bank: 1ATP), which is conserved in serine/threonine kinases. (*b*) ADP- and ATP-desthiobiotin probes acylate the kinase catalytic lysine and other ATP-proximal lysines in cell lysates. Chemical structures of (*c*) 5′-fluorosulfonylbenzoyl adenosine (FSBA) and (*d*) clickable sulfonyl fluoride probe **2**, which potently labels SRC family kinases in cells.

Other lysines just outside the kinase active site are also modified to varying extents. The acyl phosphate probes contain a desthiobiotin moiety attached via its carboxylic acid to the β-phosphate of ADP or the γ-phosphate of ATP. A lysine in close proximity to the terminal phosphate of the reversibly bound probe attacks the carbonyl to form a stable desthiobiotin carboxamide, with expulsion of the ADP/ATP leaving group (**Figure 3*b***).

In a typical chemoproteomic profiling experiment, ATP-desthiobiotin (5 μM) is added to gel-filtered (ATP-depleted) cell lysates in the absence or presence of a competing kinase inhibitor. After exhaustive trypsinization, desthiobiotinylated peptides are enriched with streptavidin beads and analyzed by quantitative mass spectrometry. By comparing MS intensities of kinase-derived, desthiobiotinylated peptides from control versus inhibitor-treated lysates, one can estimate inhibitor occupancy of up to 150–200 endogenous kinases from a single cell line and >300 kinases across multiple cell lines (40, 62–68). Reproducible detection and quantification of hundreds of unique kinases—each of which can contribute only 1 or 2 probe-modified peptides—requires a significant time investment to develop a robust mass spectrometry pipeline (69–71). In addition to kinases, ADP- and ATP-desthiobiotin probes covalently modify hundreds of nonkinase proteins, including HSP70 and HSP90 chaperones, in an ATP-competitive manner (72).

Sulfonyl fluorides react with multiple protein nucleophiles, yet they are relatively stable to hydrolysis at physiological pH (73–75). Reactions with amines and hydroxyls (lysine, tyrosine, serine, threonine) produce stable sulfonamides and sulfonates, whereas reactions with thiols and imidazoles (cysteine, histidine) result in adducts that may be labile and difficult to isolate (75–78). Sulfonyl fluorides have been used extensively as serine hydrolase inhibitors and nucleoside-based affinity probes for myriad enzymes. However, there are relatively few examples of sulfonyl fluoride probes designed to target a specific lysine in a protein active site.

5′-Fluorosulfonylbenzoyl adenosine (FSBA) binds the ATP site of numerous proteins, including protein kinases, with affinities ranging from high micromolar to low millimolar (**Figure 3*c***). Although FSBA selectively modifies the catalytic lysine of purified protein kinases (79), its utility as a chemoproteomic kinase probe is limited. To enable covalent lysine-targeted kinase inhibition in cells, we designed the sulfonyl fluoride probe **2** (**Figure 3*d***), a hybrid of FSBA and the potent SRC family kinase inhibitor, PP1 (25). The *p*-tolyl group on its pyrrolopyrimidine core was designed to fill a hydrophobic pocket in SRC and other kinases with a small amino acid at the gatekeeper position, thereby increasing the affinity by ∼10,000-fold relative to FSBA. It also contains a 2′-propargyl ether, enabling copper-catalyzed click conjugation to biotin or rhodamine azides. Probe **2** rapidly labeled SRC in live cells at nanomolar concentrations (IC_{50} ∼ 300 nM), and labeling was not observed when the catalytic lysine was mutated to arginine.

To expand the number of endogenous kinases amenable to detection by cell-permeable sulfonyl fluoride probes, we designed XO44, which links a phenylsulfonyl fluoride to a highly promiscuous kinase-binding scaffold (**Figure 4*a***) (24). Covalent modification of the catalytic lysine was revealed by cocrystal structures of XO44 bound to SRC and EGFR (**Figure 4*b***). When added to live cells, XO44 modified 133 endogenous kinases, as revealed by mass spectrometry analysis (**Figure 4*c***). This finding represents by far the largest fraction of the kinome labeled by a single probe in live cells. Using XO44 and label-free quantitative mass spectrometry, we observed selective engagement of endogenous ABL1, BLK, SRC, and LCK by clinically relevant concentrations of the myeloid leukemia drug, dasatinib.

A remarkable feature of XO44, as shown by chemoproteomic analysis, is its selective promiscuity. Other than protein kinases, most of which were labeled to saturation by XO44 within 30 min, very few proteins were specifically enriched and identified by mass spectrometry. These results suggest that sulfonyl fluorides such as XO44 occupy a sweet spot in electrophile space, efficiently reacting with an appropriately positioned lysine while reacting slowly with most

Annu. Rev. Biochem. 2019.88:365-381. Downloaded from www.annualreviews.org
Access provided by University of California - San Francisco UCSF on 06/24/19. For personal use only.

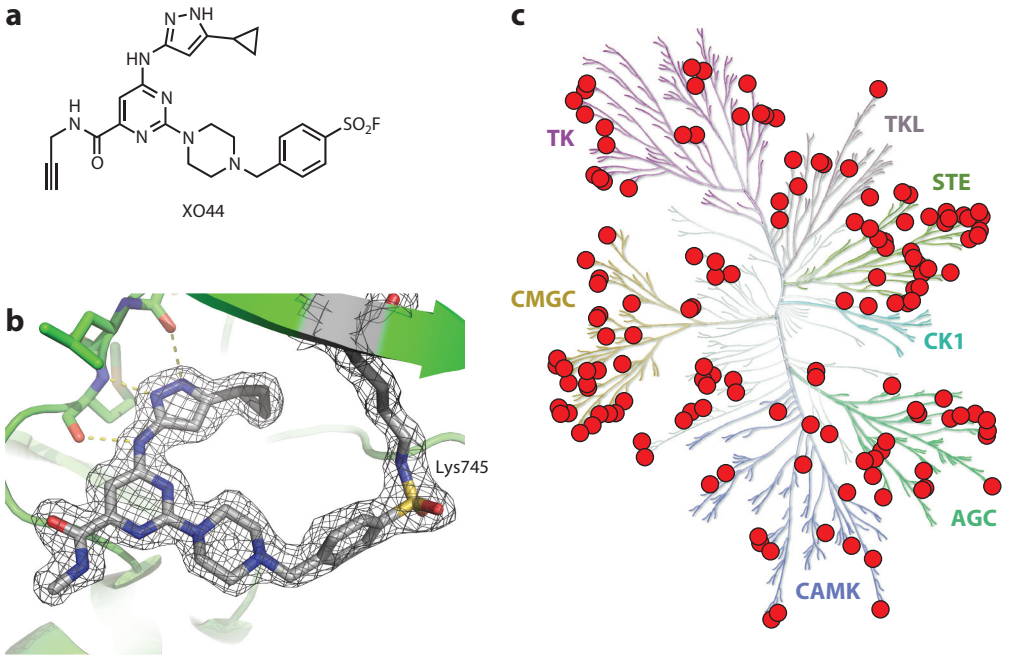

Figure 4

XO44, a broad-spectrum probe for quantifying kinase occupancy in living cells. (*a*) Chemical structure of XO44, comprising an aminopyrazole noncovalent kinase-recognition moiety, a piperazine linker, and a phenylsulfonyl fluoride. (*b*) Crystal structure of XO44 covalently bound to the EGFR kinase domain (Protein Data Bank: 5U8L) (24). (*c*) Kinase dendrogram showing kinases covalently labeled by XO44 in Jurkat cells. Figure adapted with permission from Reference 24; copyright 2017 American Chemical Society.

off-target nucleophiles when added to cells at low micromolar concentrations. As mentioned above, sulfonyl fluoride probes have been designed to target other protein nucleophiles, including a tyrosine in the mRNA decapping enzyme, DCPS (80). In the case of DCPS, a lysine is within 7 Å of the modified tyrosine. It remains to be determined which specific features in the protein microenvironment favor sulfonyl fluoride modification of tyrosine versus lysine.

TARGETING NONCATALYTIC LYSINES AND N-TERMINAL AMINES WITH REVERSIBLE COVALENT INHIBITORS

Reversible covalent inhibitors have the potential to exhibit sustained target engagement, high selectivity, and a reduced propensity to form adducts with off-target nucleophiles. An example of this approach is provided by cyanoacrylamide-based kinase inhibitors, which covalently modify a noncatalytic cysteine proximal to the ATP binding site (81–84). Imine (Schiff base) formation between an aldehyde-containing small molecule and a protein-derived amine—either a lysine ε-amine or an unblocked amino terminus—represents a conceptually related strategy for developing reversible covalent inhibitors with potential application to proteins that lack a suitably positioned cysteine. In this section, we highlight three recent examples of *ortho*-substituted benzaldehydes that form an imine with a specific amine on their protein target.

The *o*-hydroxy benzaldehyde (salicylaldehyde) GBT440 is in late-stage clinical development for sickle cell disease. GBT440 (also called voxelotor) forms an imine with the N-terminal amine of α-hemoglobin (**Figure 5*a***), stabilizing the oxygen-bound state and preventing polymerization

Annu. Rev. Biochem. 2019.88:365-381. Downloaded from www.annualreviews.org
Access provided by University of California - San Francisco UCSF on 06/24/19. For personal use only.

Annu. Rev. Biochem. 2019.88:365-381. Downloaded from www.annualreviews.org
Access provided by University of California - San Francisco UCSF on 06/24/19. For personal use only.

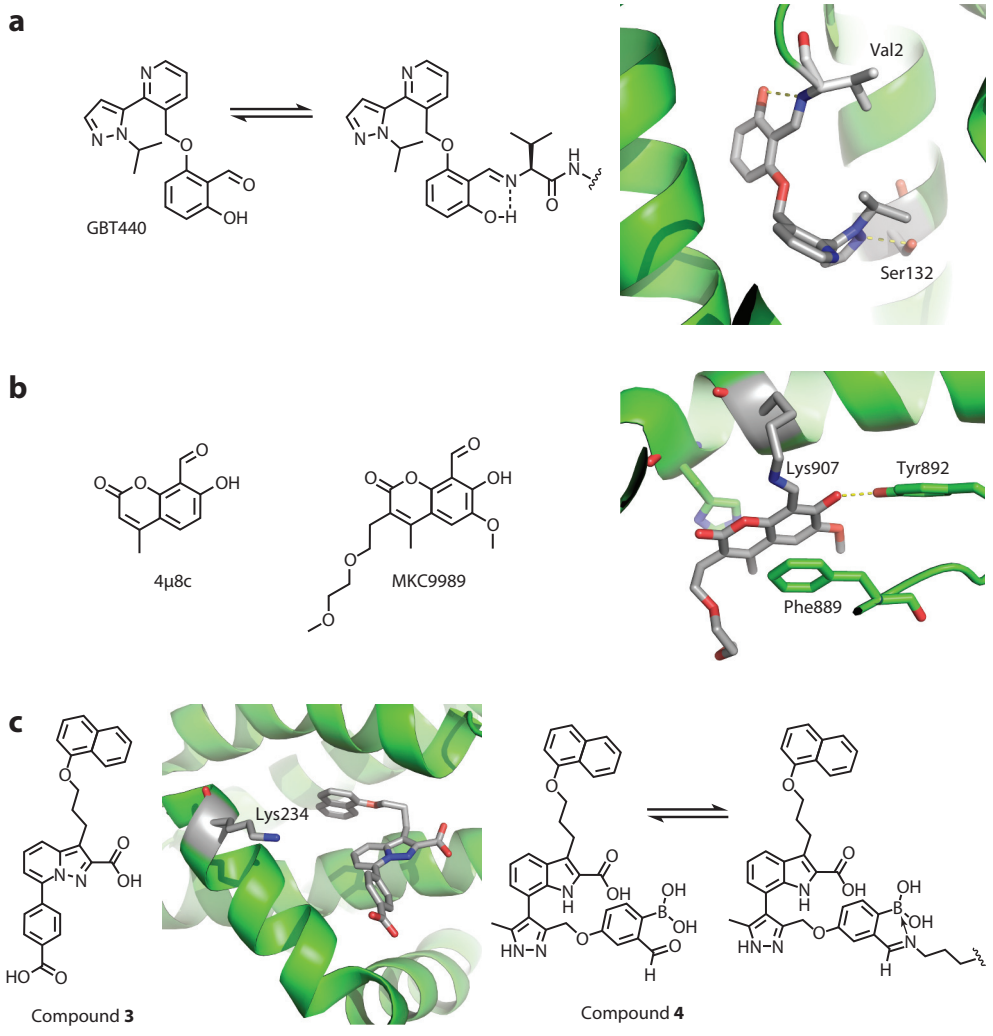

Figure 5

Targeting lysine and N-terminal amines with *ortho*-substituted aldehydes. (*a*) Salicylaldehyde inhibitor GBT440 forms a reversible imine with the N-terminal amine (Val2) of α-hemoglobin [Protein Data Bank (PDB): 5E83]. An intramolecular hydrogen bond may stabilize the covalent adduct. (*b*) Salicylaldehyde inhibitors 4μ8C and MKC9989 reversibly target Lys907 in the RNAse domain of IRE1 (PDB: 4PL3). The imine is shielded from solvent by Phe889. (*c*) The crystal structure of compound **3** bound to MCL1 (PDB: 3WIX) guided the design of *o*-boronic acid benzaldehyde **4**, a reversible covalent MCL1 inhibitor that targets Lys234.

of mutant α/β-hemoglobin tetramers (85). GBT440 analogs that lack the aldehyde are inactive, whereas those that lack the *o*-hydroxyl are less potent in vitro and show reduced erythrocyte occupancy in vivo (43). The crystal structure of GBT440 bound to the $\alpha_2\beta_2$ hemoglobin tetramer reveals an intramolecular hydrogen bond between the *o*-hydroxyl and the imine nitrogen (**Figure 5*a***), which may contribute to GBT440's long residence time in vivo. Kinetic studies of model benzaldehyde-derived imines have shown that an *o*-hydroxy group decreases the hydrolysis rate by at least 40-fold compared with an *o*-methoxy or *m*-hydroxy group (86). This profound kinetic stabilization effect has been attributed to intramolecular hydrogen bonding (**Figure 5*a***). Similar trends have been observed in kinetic measurements of transimination reactions comparing

benzaldehyde- versus salicylaldehyde-derived imines (87). GBT440 also forms an intermolecular hydrogen bond between a pyrazole nitrogen and Ser132 on the second α-chain as well as hydrophobic interactions on both sides of the α-hemoglobin dimer interface. These interactions prevent binding of a second GBT440 molecule to the symmetry-related site; this differs from earlier hemoglobin stabilizers, most of which bind with 2:1 stoichiometry (88–90). Hence, similar to cysteine-targeted reversible covalent kinase inhibitors (81, 84), covalent and noncovalent interactions cooperatively stabilize a long-lived complex between GBT440 and the hemoglobin tetramer.

Salicylaldehydes (and salicylaldimines) have also been discovered to inhibit the unconventional RNA splicing activity of IRE1 (91, 92), a transmembrane protein kinase and RNAse that signals in response to unfolded protein accumulation in the endoplasmic reticulum. Compound 4μ8c (8-formyl-7-hydroxy-4-methylcoumarin) and other related salicylaldehydes form reversible imines with Lys907, a noncatalytic lysine in the RNAse domain of IRE1 (**Figure 5*b***) (44). Benzaldehydes that lack the *o*-hydroxyl group are inactive (45, 92). Molecular dynamics simulations suggest that Lys907 has a shifted pK_a of ∼7 (compared with a pK_a of 10–11 for fully solvated lysine) (93). Lys907 is buried in a hydrophobic pocket and shielded from solvent, potentially contributing to its decreased pK_a and increased nucleophilicity. Crystal structures of IRE1 bound to salicylaldehyde inhibitors confirm imine formation with Lys907 (45), but the orientation of the imine nitrogen precludes intramolecular hydrogen bonding (**Figure 5*b***). Instead, the *o*-hydroxyl forms a hydrogen bond with the catalytically essential Tyr892. The imine is further shielded from solvent by a pi-stacking interaction with Phe889. Solvent accessibility of the imine—which must undergo nucleophilic attack by a water molecule prior to dissociation of the inhibitor—is likely a major determinant of residence time for amine-targeted aldehyde inhibitors, in addition to intra- and intermolecular stabilizing interactions.

The salicylaldehyde-based ligands described above provide evidence that a hydroxyl substituent *ortho* to the electrophilic aldehyde can have a profound impact on potency. A similar concept, based on intramolecular imine stabilization, was employed in the design of benzaldehydes (and acetophenones) with an *o*-boronic acid substituent. *o*-Boronic acid aldehydes react with amines to form iminoboronates, whose thermodynamic stability is thought to derive from an intramolecular dative bond between the imine nitrogen and boron (46) or an ionic interaction between the protonated imine and the negatively charged boronate (94). Starting with the noncovalent ligand **3**, *o*-boronic acid aldehyde **4** was designed to target a noncatalytic surface lysine (Lys234) near the BH3 binding groove of MCL1, an antiapoptotic regulator that promotes cancer cell survival (47) (**Figure 5*c***). Compound **4** binds MCL1 tightly (IC_{50} ∼ 5 nM), and mutation of Lys234 to alanine results in a 30-fold reduction in binding affinity. Both the aldehyde and the boronic acid are critical for potency, as analogs lacking either exhibit from 20- to 50-fold lower binding affinity for MCL1 and >20-fold lower cellular potency. Compared with cysteine-targeted reversible covalent kinase inhibitors with residence times of hours to days (81, 84), *o*-boronic acid aldehyde **4** dissociates from MCL1 much faster ($t_{1/2}$ ∼ 38 s). Only limited kinetic data are available for other amine-targeted aldehyde-based inhibitors, including the salicylaldehyde ligands for IRE1 and hemoglobin described above. In this regard, it would be of interest to directly compare the hydrolysis rates of model imines (in pH ∼ 7 buffer) and protein/ligand adducts derived from *o*-boronic acid aldehydes, salicylaldehydes, and other substituted benzaldehydes.

In summary, aldehyde-based covalent inhibitors—in particular, salicylaldehydes and *o*-boronic acid benzaldehydes—have been designed or discovered to reversibly target an amine (N-terminal amine or lysine ε-amine) proximal to a ligand binding site on α-hemoglobin (allosteric site), IRE1 (RNAse active site), and MCL1 (protein–protein interaction site). The affinity, selectivity, and residence time are likely determined by a combination of tunable properties, including the

Annu. Rev. Biochem. 2019.88:365-381. Downloaded from www.annualreviews.org
Access provided by University of California - San Francisco UCSF on 06/24/19. For personal use only.

intrinsic stability of the product imine—its solvent accessibility, bound conformation, and ability to form intramolecular interactions—as well as noncovalent intermolecular interactions between the ligand and the protein. It should be possible to optimize these cooperative stabilizing interactions by structure-based design. Moreover, the strategy of targeting lysines and N-terminal amines with reversible covalent inhibitors should be applicable to any target with a suitably reactive amine proximal to a ligand binding site.

CONCLUSIONS AND PERSPECTIVE

Broad application of covalent inhibitors and probes to protein sites that lack a ligandable cysteine requires new approaches in medicinal chemistry, chemical biology, and chemoproteomics. The total number of proteins with a ligandable lysine is currently unknown. Nevertheless, our analysis of the PDB suggests that the majority of enzyme cofactor binding sites—and perhaps by extension, other ligand binding sites—contain at least one proximal lysine. Although quantitative chemoproteomic studies have begun to reveal the reactivity and ligandability of lysines on a proteome-wide scale (41, 42), we argue that the amine-reactive probes deployed thus far have captured only a small fraction of the ligandable lysinome, implied by the absence of many active-site lysines in published chemoproteomic data sets. Key unanswered questions for future research include the following: Which lysines can efficiently capture a proximal electrophile in living cells and animals, and which electrophile is best suited for a given lysine? Innovative chemistry for the discovery of new electrophiles and their precise installation onto diverse noncovalent recognition scaffolds will play a critical role in the expansive application of covalent inhibitors and chemoproteomic probes to lysines as well as other protein nucleophiles like tyrosine, serine, and histidine. Finally, advances in multiplexed quantitative mass spectrometry and chemoproteomic probe design are required to fully explore the vast uncharted universe of ligandable protein nucleophiles in cells and organisms.

DISCLOSURE STATEMENT

J.T. is a cofounder and shareholder of Global Blood Therapeutics, Principia Biopharma, Kezar Life Sciences, and Cedilla Therapeutics.

ACKNOWLEDGMENTS

We thank members of the Taunton laboratory, including Geoff Smith, Phillip Sharp, and Jordan Carelli, for comments on the manuscript. This work was supported by Pfizer (J.T.) and the National Cancer Institute (A.C.; grant number F31CA214028).

LITERATURE CITED

1. Baillie TA. 2016. Targeted covalent inhibitors for drug design. *Angew. Chem. Int. Ed. Engl.* 55:13408–21
2. Jones LH. 2018. Reactive chemical probes: beyond the kinase cysteinome. *Angew. Chem. Int. Ed. Engl.* 57:9220–23
3. Copeland RA, Pompliano DL, Meek TD. 2006. Drug-target residence time and its implications for lead optimization. *Nat. Rev. Drug Discov.* 5:730–39
4. Copeland RA. 2016. The drug-target residence time model: a 10-year retrospective. *Nat. Rev. Drug Discov.* 15:87–95
5. Moellering RE, Cravatt BF. 2012. How chemoproteomics can enable drug discovery and development. *Chem. Biol.* 19:11–22

Annu. Rev. Biochem. 2019.88:365-381. Downloaded from www.annualreviews.org
Access provided by University of California - San Francisco UCSF on 06/24/19. For personal use only.

6. Ostrem JM, Peters U, Sos ML, Wells JA, Shokat KM. 2013. K-Ras(G12C) inhibitors allosterically control GTP affinity and effector interactions. *Nature* 503:548–51
7. Lito P, Solomon M, Li LS, Hansen R, Rosen N. 2016. Allele-specific inhibitors inactivate mutant KRAS G12C by a trapping mechanism. *Science* 351:604–8
8. Van Neck T, Pannecouque C, Vanstreels E, Stevens M, Dehaen W, Daelemans D. 2008. Inhibition of the CRM1-mediated nucleocytoplasmic transport by N-azolylacrylates: structure-activity relationship and mechanism of action. *Bioorg. Med. Chem.* 16:9487–97
9. Neggers JE, Vercruysse T, Jacquemyn M, Vanstreels E, Baloglu E, et al. 2015. Identifying drug-target selectivity of small-molecule CRM1/XPO1 inhibitors by CRISPR/Cas9 genome editing. *Chem. Biol.* 22:107–16
10. Patricelli MP, Janes MR, Li L-S, Hansen R, Peters U, et al. 2016. Selective inhibition of oncogenic KRAS output with small molecules targeting the inactive state. *Cancer Discov.* 6:316–29
11. Walker CJ, Oaks JJ, Santhanam R, Neviani P, Harb JG, et al. 2013. Preclinical and clinical efficacy of XPO1/CRM1 inhibition by the karyopherin inhibitor KPT-330 in Ph+ leukemias. *Blood* 122:3034–44
12. Lapalombella R, Sun Q, Williams K, Tangeman L, Jha S, et al. 2012. Selective inhibitors of nuclear export show that CRM1/XPO1 is a target in chronic lymphocytic leukemia. *Blood* 120:4621–34
13. Miller RM, Taunton J. 2014. Targeting protein kinases with selective and semipromiscuous covalent inhibitors. *Methods Enzymol.* 548:93–116
14. Liu Q, Sabnis Y, Zhao Z, Zhang T, Buhrlage SJ, et al. 2013. Developing irreversible inhibitors of the protein kinase cysteinome. *Chem. Biol.* 20:146–59
15. Singh J, Petter RC, Kluge AF. 2010. Targeted covalent drugs of the kinase family. *Curr. Opin. Chem. Biol.* 14:475–80
16. Barf T, Kaptein A. 2012. Irreversible protein kinase inhibitors: balancing the benefits and risks. *J. Med. Chem.* 55:6243–62
17. Li D, Ambrogio L, Shimamura T, Kubo S, Takahashi M, et al. 2008. BIBW2992, an irreversible EGFR/HER2 inhibitor highly effective in preclinical lung cancer models. *Oncogene* 27:4702–11
18. Cross DAE, Ashton SE, Ghiorghiu S, Eberlein C, Nebhan CA, et al. 2014. AZD9291, an irreversible EGFR TKI, overcomes T790M-mediated resistance to EGFR inhibitors in lung cancer. *Cancer Discov.* 4:1046–61
19. Honigberg LA, Smith AM, Sirisawad M, Verner E, Loury D, et al. 2010. The Bruton tyrosine kinase inhibitor PCI-32765 blocks B-cell activation and is efficacious in models of autoimmune disease and B-cell malignancy. *PNAS* 107:13075–80
20. Rabindran SK, Discafani CM, Rosfjord EC, Baxter M, Floyd MB, et al. 2004. Antitumor activity of HKI-272, an orally active, irreversible inhibitor of the HER-2 tyrosine kinase. *Cancer Res.* 64:3958–65
21. Byrd JC, Harrington B, O'Brien S, Jones JA, Schuh A, et al. 2016. Acalabrutinib (ACP-196) in relapsed chronic lymphocytic leukemia. *N. Engl. J. Med.* 374:323–32
22. Grimster NP, Connelly S, Baranczak A, Dong J, Krasnova LB, et al. 2013. Aromatic sulfonyl fluorides covalently kinetically stabilize transthyretin to prevent amyloidogenesis while affording a fluorescent conjugate. *J. Am. Chem. Soc.* 135:5656–68
23. Hoppmann C, Wang L. 2016. Proximity-enabled bioreactivity to generate covalent peptide inhibitors of p53–Mdm4. *Chem. Commun.* 52:5140–43
24. Zhao Q, Ouyang X, Wan X, Gajiwala KS, Kath JC, et al. 2017. Broad-spectrum kinase profiling in live cells with lysine-targeted sulfonyl fluoride probes. *J. Am. Chem. Soc.* 139:680–85
25. Gushwa NN, Kang S, Chen J, Taunton J. 2012. Selective targeting of distinct active site nucleophiles by irreversible SRC-family kinase inhibitors. *J. Am. Chem. Soc.* 134:20214–17
26. Baranczak A, Liu Y, Connelly S, Du W-GH, Greiner ER, et al. 2015. A fluorogenic aryl fluorosulfate for intraorganellar transthyretin imaging in living cells and in *Caenorhabditis elegans*. *J. Am. Chem. Soc.* 137:7404–14
27. Mortenson DE, Brighty GJ, Plate L, Bare G, Chen W, et al. 2018. "Inverse drug discovery" strategy to identify proteins that are targeted by latent electrophiles as exemplified by aryl fluorosulfates. *J. Am. Chem. Soc.* 140:200–10

Annu. Rev. Biochem. 2019.88:365-381. Downloaded from www.annualreviews.org
Access provided by University of California - San Francisco UCSF on 06/24/19. For personal use only.

28. Ihle NT, Williams R, Chow S, Chew W, Berggren MI, et al. 2004. Molecular pharmacology and antitumor activity of PX-866, a novel inhibitor of phosphoinositide-3-kinase signaling. *Mol. Cancer Ther.* 3:763–72
29. Anscombe E, Meschini E, Mora-Vidal R, Martin MP, Staunton D, et al. 2015. Identification and characterization of an irreversible inhibitor of CDK2. *Chem. Biol.* 22:1–6
30. Manglik A, Kruse AC, Kobilka TS, Thian FS, Mathiesen JM, et al. 2012. Crystal structure of the μ-opioid receptor bound to a morphinan antagonist. *Nature* 485:321–26
31. Suh EH, Liu Y, Connelly S, Genereux JC, Wilson IA, Kelly JW. 2013. Stilbene vinyl sulfonamides as fluorogenic sensors of and traceless covalent kinetic stabilizers of transthyretin that prevent amyloidogenesis. *J. Am. Chem. Soc.* 135:17869–80
32. Pettinger J, Le Bihan YV, Widya M, van Montfort RLM, Jones K, Cheeseman MD. 2017. An irreversible inhibitor of HSP72 that unexpectedly targets lysine-56. *Angew. Chem. Int. Ed. Engl.* 56:3536–40
33. Mohamed MS, Larson DL, Takemori AE, Portoghese PS. 1986. Activity of N-methyl-α- and -β-funaltrexamine at opioid receptors. *J. Med. Chem.* 29:1551–53
34. Shannon DA, Banerjee R, Webster ER, Bak DW, Wang C, Weerapana E. 2014. Investigating the proteome reactivity and selectivity of aryl halides. *J. Am. Chem. Soc.* 136:3330–33
35. Choi S, Connelly S, Reixach N, Wilson IA, Kelly JW. 2010. Chemoselective small molecules that covalently modify one lysine in a non-enzyme protein in plasma. *Nat. Chem. Biol.* 6:133–39
36. Tamura T, Ueda T, Goto T, Tsukidate T, Shapira Y, et al. 2018. Rapid labelling and covalent inhibition of intracellular native proteins using ligand-directed *N*-acyl-*N*-alkyl sulfonamide. *Nat. Commun.* 9:1–12
37. Dalton SE, Dittus L, Thomas DA, Convery MA, Nunes J, et al. 2018. Selectively targeting the kinome-conserved lysine of PI3Kδ as a general approach to covalent kinase inhibition. *J. Am. Chem. Soc.* 140:932–39
38. Yasueda Y, Tamura T, Fujisawa A, Kuwata K, Tsukiji S, et al. 2016. A set of organelle-localizable reactive molecules for mitochondrial chemical proteomics in living cells and brain tissues. *J. Am. Chem. Soc.* 138:7592–602
39. Patricelli MP, Szardenings AK, Liyanage M, Nomanbhoy TK, Wu M, et al. 2007. Functional interrogation of the kinome using nucleotide acyl phosphates. *Biochemistry* 46:350–58
40. Patricelli MP, Nomanbhoy TK, Wu J, Brown H, Zhou D, et al. 2011. In situ kinase profiling reveals functionally relevant properties of native kinases. *Chem. Biol.* 18:699–710
41. Hacker SM, Backus KM, Lazear MR, Forli S, Correia BE, Cravatt BF. 2017. Global profiling of lysine reactivity and ligandability in the human proteome. *Nat. Chem.* 9:1181–90
42. Ward CC, Kleinman JI, Nomura DK. 2017. NHS-esters as versatile reactivity-based probes for mapping proteome-wide ligandable hotspots. *ACS Chem. Biol.* 12:1478–83
43. Metcalf B, Chuang C, Dufu K, Patel MP, Silva-Garcia A, et al. 2017. Discovery of GBT440, an orally bioavailable R-state stabilizer of sickle cell hemoglobin. *ACS Med. Chem. Lett.* 8:321–26
44. Cross BCS, Bond PJ, Sadowski PG, Jha BK, Zak J, et al. 2012. The molecular basis for selective inhibition of unconventional mRNA splicing by an IRE1-binding small molecule. *PNAS* 109:E869–78
45. Sanches M, Duffy NM, Talukdar M, Thevakumaran N, Chiovitti D, et al. 2014. Structure and mechanism of action of the hydroxy-aryl-aldehyde class of IRE1 endoribonuclease inhibitors. *Nat. Commun.* 5:1–16
46. Cal PMSD, Vicente JB, Pires E, Coelho AV, Veiros LF, et al. 2012. Iminoboronates: a new strategy for reversible protein modification. *J. Am. Chem. Soc.* 134:10299–305
47. Akçay G, Belmonte MA, Aquila B, Chuaqui C, Hird AW, et al. 2016. Inhibition of Mcl-1 through covalent modification of a noncatalytic lysine side chain. *Nat. Chem. Biol.* 12:931–36
48. Pettinger J, Jones K, Cheeseman MD. 2017. Lysine-targeting covalent inhibitors. *Agnew. Chem. Int. Ed. Eng.* 56:15200–9
49. Aksnes H, Drazic A, Marie M, Arnesen T. 2016. First things first: vital protein marks by N-terminal acetyltransferases. *Trends Biochem. Sci.* 41:746–60
50. Vu LP, Pickering BF, Cheng Y, Zaccara S, Nguyen D, et al. 2017. The N^6-methyladenosine (m^6A)-forming enzyme METTL3 controls myeloid differentiation of normal hematopoietic and leukemia cells. *Nat. Med.* 23:1369–76

Annu. Rev. Biochem. 2019.88:365-381. Downloaded from www.annualreviews.org
Access provided by University of California - San Francisco UCSF on 06/24/19. For personal use only.

51. Wang X, Feng J, Xue Y, Guan Z, Zhang D, et al. 2016. Structural basis of N^6-adenosine methylation by the METTL3–METTL14 complex. *Nature* 534:575–78
52. Isom DG, Castañeda CA, Cannon BR, García-Moreno E B. 2011. Large shifts in pKa values of lysine residues buried inside a protein. *PNAS* 108:5260–65
53. Baeza J, Smallegan MJ, Denu JM. 2015. Site-specific reactivity of nonenzymatic lysine acetylation. *ACS Chem. Biol.* 10:122–28
54. Cardote TAF, Gadd MS, Ciulli A. 2017. Crystal structure of the Cul2-Rbx1-EloBC-VHL ubiquitin ligase complex. *Structure* 25:901–11
55. Schneekloth JS, Fonseca FN, Koldobskiy M, Mandal A, Deshaies R, et al. 2004. Chemical genetic control of protein levels: selective in vivo targeted degradation. *J. Am. Chem. Soc.* 126:3748–54
56. Sakamoto KM, Kim KB, Kumagai A, Mercurio F, Crews CM, Deshaies RJ. 2001. Protacs: chimeric molecules that target proteins to the Skp1–Cullin–F box complex for ubiquitination and degradation. *PNAS* 98:8554–59
57. Winter GE, Buckley DL, Paulk J, Roberts JM, Souza A, et al. 2015. Phthalimide conjugation as a strategy for in vivo target protein degradation. *Science* 348:1376–81
58. Lai AC, Crews CM. 2016. Induced protein degradation: an emerging drug discovery paradigm. *Nat. Rev. Drug Discov.* 16:101–14
59. Smith GA, Uchida K, Weiss A, Taunton J. 2016. Essential biphasic role for JAK3 catalytic activity in IL-2 receptor signaling. *Nat. Chem. Biol.* 12:373–79
60. Bantscheff M, Eberhard D, Abraham Y, Bastuck S, Boesche M, et al. 2007. Quantitative chemical proteomics reveals mechanisms of action of clinical ABL kinase inhibitors. *Nat. Biotechnol.* 25:1035–44
61. Savitski MM, Reinhard FBM, Franken H, Werner T, Savitski MF, et al. 2014. Tracking cancer drugs in living cells by thermal profiling of the proteome. *Science* 346:1255784
62. Xie T, Lim SM, Westover KD, Dodge ME, Ercan D, et al. 2014. Pharmacological targeting of the pseudokinase Her3. *Nat. Chem. Biol.* 10:1006–12
63. Zhang T, Kwiatkowski N, Olson CM, Dixon-Clarke SE, Abraham BJ, et al. 2016. Covalent targeting of remote cysteine residues to develop CDK12 and CDK13 inhibitors. *Nat. Chem. Biol.* 12:876–84
64. Kwiatkowski N, Zhang T, Rahl PB, Abraham BJ, Reddy J, et al. 2014. Targeting transcription regulation in cancer with a covalent CDK7 inhibitor. *Nature* 511:616–20
65. Tan L, Nomanbhoy T, Gurbani D, Patricelli M, Hunter J, et al. 2015. Discovery of type II inhibitors of TGFβ-activated kinase 1 (TAK1) and mitogen-activated protein kinase kinase kinase kinase 2 (MAP4K2). *J. Med. Chem.* 58:183–96
66. Matthews JM, Bhatt S, Patricelli MP, Nomanbhoy TK, Jiang X, et al. 2016. Pathophysiological significance and therapeutic targeting of germinal center kinase in diffuse large B-cell lymphoma. *Blood* 128:239–48
67. Yang Q, Deng X, Lu B, Cameron M, Fearns C, et al. 2010. Pharmacological inhibition of BMK1 suppresses tumor growth through promyelocytic leukemia protein. *Cancer Cell* 18:258–67
68. Ronan B, Flamand O, Vescovi L, Dureuil C, Durand L, et al. 2014. A highly potent and selective Vps34 inhibitor alters vesicle trafficking and autophagy. *Nat. Chem. Biol.* 10:1013–19
69. Xiao Y, Guo L, Wang Y. 2014. A targeted quantitative proteomics strategy for global kinome profiling of cancer cells and tissues. *Mol. Cell. Proteom.* 13:1065–75
70. Worboys JD, Sinclair J, Yuan Y, Jørgensen C. 2014. Systematic evaluation of quantotypic peptides for targeted analysis of the human kinome. *Nat. Methods* 11:1041–44
71. McAllister FE, Niepel M, Haas W, Huttlin E, Sorger PK, Gygi SP. 2013. Mass spectrometry based method to increase throughput for kinome analyses using ATP probes. *Anal. Chem.* 85:4666–74
72. Nordin BE, Liu Y, Aban A, Brown HE, Wu J, et al. 2015. ATP acyl phosphate reactivity reveals native conformations of Hsp90 paralogs and inhibitor target engagement. *Biochemistry* 54:3024–36
73. Gardner Swain C, Scott CB. 1953. Rates of solvolysis of some alkyl fluorides and chlorides. *J. Am. Chem. Soc.* 75:246–48
74. Dong J, Krasnova L, Finn MG, Sharpless KB. 2014. Sulfur(VI) fluoride exchange (SuFEx): another good reaction for click chemistry. *Angew. Chem. Int. Ed. Engl.* 53:9430–48

Annu. Rev. Biochem. 2019.88:365-381. Downloaded from www.annualreviews.org
Access provided by University of California - San Francisco UCSF on 06/24/19. For personal use only.

75. Narayanan A, Jones LH. 2015. Sulfonyl fluorides as privileged warheads in chemical biology. *Chem. Sci.* 6:2650–59
76. Ciuffarin E, Senatore L, Isola M. 1972. Nucleophilic substitution at four coordinate sulphur. Mobility of the leaving group. *J. Chem. Soc. Perkin Trans. 2* 0:468–71
77. Aberlin ME, Bunton CA. 1970. The spontaneous hydrolysis of sulfonyl fluorides. *J. Org. Chem.* 35:1825–28
78. Mukherjee H, Debreczeni J, Breed J, Tentarelli S, Aquila B, et al. 2017. A study of the reactivity of S(VI)-F containing warheads with nucleophilic amino-acid side chains under physiological conditions. *Org. Biomol. Chem.* 15:9685–95
79. Zoller MJ, Taylor SS. 1979. Affinity labeling of the nucleotide binding site of the catalytic subunit of cAMP-dependent protein kinase site using *p*-fluorosulfonyl-[^{14}C]benzoyl 5′-adenosine. *J. Biol. Chem.* 254:8363–68
80. Hett EC, Xu H, Geoghegan KF, Gopalsamy A, Kyne RE, et al. 2015. Rational targeting of active-site tyrosine residues using sulfonyl fluoride probes. *ACS Chem. Biol.* 10:1094–98
81. Serafimova IM, Pufall MA, Krishnan S, Duda K, Cohen MS, et al. 2012. Reversible targeting of noncatalytic cysteines with chemically tuned electrophiles. *Nat. Chem. Biol.* 8:471–76
82. Miller RM, Paavilainen VO, Krishnan S, Serafimova IM, Taunton J. 2013. Electrophilic fragment-based design of reversible covalent kinase inhibitors. *J. Am. Chem. Soc.* 135:5298–301
83. Krishnan S, Miller RM, Tian B, Mullins RD, Jacobson MP, Taunton J. 2014. Design of reversible, cysteine-targeted Michael acceptors guided by kinetic and computational analysis. *J. Am. Chem. Soc.* 136:12624–30
84. Bradshaw JM, McFarland JM, Paavilainen VO, Bisconte A, Tam D, et al. 2015. Prolonged and tunable residence time using reversible covalent kinase inhibitors. *Nat. Chem. Biol.* 11:525–31
85. Oksenberg D, Dufu K, Patel MP, Chuang C, Li Z, et al. 2016. GBT440 increases haemoglobin oxygen affinity, reduces sickling and prolongs RBC half-life in a murine model of sickle cell disease. *Br. J. Haematol.* 175:141–53
86. Bruyneel W, Charette JJ, De Hoffmann E. 1966. Kinetics of hydrolysis of hydroxy and methoxy derivatives of N-benzylidene-2-aminopropane. *J. Am. Chem. Soc.* 88:3808–13
87. Kovaříček P, Lehn JM. 2012. Merging constitutional and motional covalent dynamics in reversible imine formation and exchange processes. *J. Am. Chem. Soc.* 134:9446–55
88. Wireko FC, Abraham DJ. 1991. X-ray diffraction study of the binding of the antisickling agent 12C79 to human hemoglobin. *PNAS* 88:2209–11
89. Safo MK, Abdulmalik O, Danso-Danquah R, Burnett JC, Nokuri S, et al. 2004. Structural basis for the potent antisickling effect of a novel class of five-membered heterocyclic aldehydic compounds. *J. Med. Chem.* 47:4665–76
90. Abdulmalik O, Ghatge MS, Musayev FN, Parikh A, Chen Q, et al. 2011. Crystallographic analysis of human hemoglobin elucidates the structural basis of the potent and dual antisickling activity of pyridyl derivatives of vanillin. *Acta Crystallogr. Sect. D* D67:920–28
91. Papandreou I, Denko NC, Olson M, Van Melckebeke H, Lust S, et al. 2011. Identification of an Ire1alpha endonuclease specific inhibitor with cytotoxic activity against human multiple myeloma. *Blood* 117:1311–14
92. Volkmann K, Lucas JL, Vuga D, Wang X, Brumm D, et al. 2011. Potent and selective inhibitors of the inositol-requiring enzyme 1 endoribonuclease. *J. Biol. Chem.* 286:12743–55
93. Tomasio SM, Harding HP, Ron D, Cross BCS, Bond PJ. 2013. Selective inhibition of the unfolded protein response: targeting catalytic sites for Schiff base modification. *Mol. Biosyst.* 9:2408–16
94. Gutiérrez-Moreno NJ, Medrano F, Yatsimirsky AK. 2012. Schiff base formation and recognition of amino sugars, aminoglycosides and biological polyamines by 2-formyl phenylboronic acid in aqueous solution. *Org. Biomol. Chem.* 10:6960–72

Annu. Rev. Biochem. 2019.88:365-381. Downloaded from www.annualreviews.org
Access provided by University of California - San Francisco UCSF on 06/24/19. For personal use only.

Annual Review of Biochemistry
Volume 88, 2019

Contents

Annu. Rev. Biochem. 2019.88:365-381. Downloaded from www.annualreviews.org
Access provided by University of California - San Francisco UCSF on 06/24/19. For personal use only.

Annu. Rev. Biochem. 2019.88:365-381. Downloaded from www.annualreviews.org
Access provided by University of California - San Francisco UCSF on 06/24/19. For personal use only.

Errata

An online log of corrections to *Annual Review of Biochemistry* articles may be found at http://www.annualreviews.org/errata/biochem

Annu. Rev. Biochem. 2019.88:365-381. Downloaded from www.annualreviews.org
Access provided by University of California - San Francisco UCSF on 06/24/19. For personal use only.